UNITED STATES DEPARTMENT OF THE INTERIOR

GEOLOGICAL SURVEY

Caldera-Related Lava Flows and Intrusions of the South-Central San Juan Mountains, Colorado--

Analytical Data

by

Douglas B. Yager[1], Peter W. Lipman[2], and David A. Sawyer[3]

Open-File Report 91-313

[1]U.S. Geological Survey
Box 25046, MS 903
Denver Federal Center
Denver, CO 80225

[2]U.S. Geological Survey
MS 910
345 Middlefield Road
Menlo Park, CA 94025

[3]U.S. Geological Survey
Box 25046, MS 913
Denver Federal Center
Denver, CO 80225

1991

CONTENTS

LIST OF FIGURES

LIST OF TABLES

CALDERA-RELATED LAVA FLOWS AND INTRUSIONS OF THE SOUTH-CENTRAL SAN JUAN MOUNTAINS, COLORADO--ANALYTICAL DATA

ABSTRACT

Petrographic, major-oxide, and trace-element data for voluminous Oligocene lava flows and associated intrusions from the southern side of the central San Juan caldera cluster, Colorado, allow subdivision of these postcaldera rocks: (1) volcanic rocks of South River Peak (mostly andesite and mafic dacite containing <63% SiO_2), spatially related to the newly recognized 27.2 Ma South River caldera (source of the Wason Park Tuff), and (2) Fisher Quartz Latite (mostly silicic dacite: >63% SiO_2), related to the 26.9 Ma Creede caldera (source of the Snowshoe Mountain Tuff). The volcanic rocks of South River Peak, previously included with the Fisher Quartz Latite, are separated because of their more mafic compositions and association with a seperate caldera cycle. In the same region, slightly older andesite-dacite volcanics of Table Mountain (27.2-27.3 Ma) are chemically distinct from the younger lavas, and these volcanics may represent post-collapse volcanism associated with the newly identified Lake Humphreys caldera (source of the 27.3 Ma tuff of Blue Creek), or, alternatively, extracaldera volcanism prior to formation of the South River caldera. The caldera-related lava flows are classified by reference to a total alkali versus silica diagram, and sample locations are shown on an accompanying generalized geologic map (scale 1:50,000).

INTRODUCTION

Large volume ash-flow sheets and associated calderas near Creede in the central San Juan volcanic field, Colorado, were initially described by Steven and Ratté (1965) and have been much studied since. Nevertheless, stratigraphic and structural relations have been clarified only recently for several of the major ash-flow sheets, associated flows, and source calderas (table 1), based on field mapping, petrologic study, $^{40/39}Ar$ geochronology, and paleomagnetic data (Lipman and others, 1989; Lanphere, 1988; R. Reynolds and J. Rosenbaum, unpubl. data, 1989). For example, the source of the 27.2 Ma Wason Park Tuff, previously inferred to be concealed beneath the Creede caldera (Ratté and Steven, 1967), has been shown to be the newly recognized South River caldera (Lipman and others, 1989). Post-collapse lava flows related to the South River and Creede calderas in the southern part of the central San Juan cluster (fig. 1) are the focus of the chemical data and brief interpretation reported here.

TABLE 1. ASH-FLOW TUFFS AND LAVAS OF THE CENTRAL SAN JUAN CALDERA CLUSTER

[Modified from Lipman and others, 1989;
$^{40/39}Ar$ ages from Lanphere, 1988 and Lanphere, unpublished data]

Tuff Unit	Source caldera	Age of Tuffs (Ma)	Post-collapse lavas
Nelson Mountain	San Luis caldera complex	26.1	Stewart Peak & Baldy Cinco
Rat Creek	San Luis caldera complex	26.5	--
Snowshoe Mountain	Creede	26.9	Fisher Quartz Latite
Wason Park	South River	27.2	Volcanic rocks of South River
Blue Creek	Lake Humphreys	27.3	Volcanics of Table Mountain?
Carpenter Ridge	Bachelor	27.4	--
Fish Canyon	La Garita	27.55	--
Masonic Park	Mount Hope	28.3	Andesite of Sheep Mountain

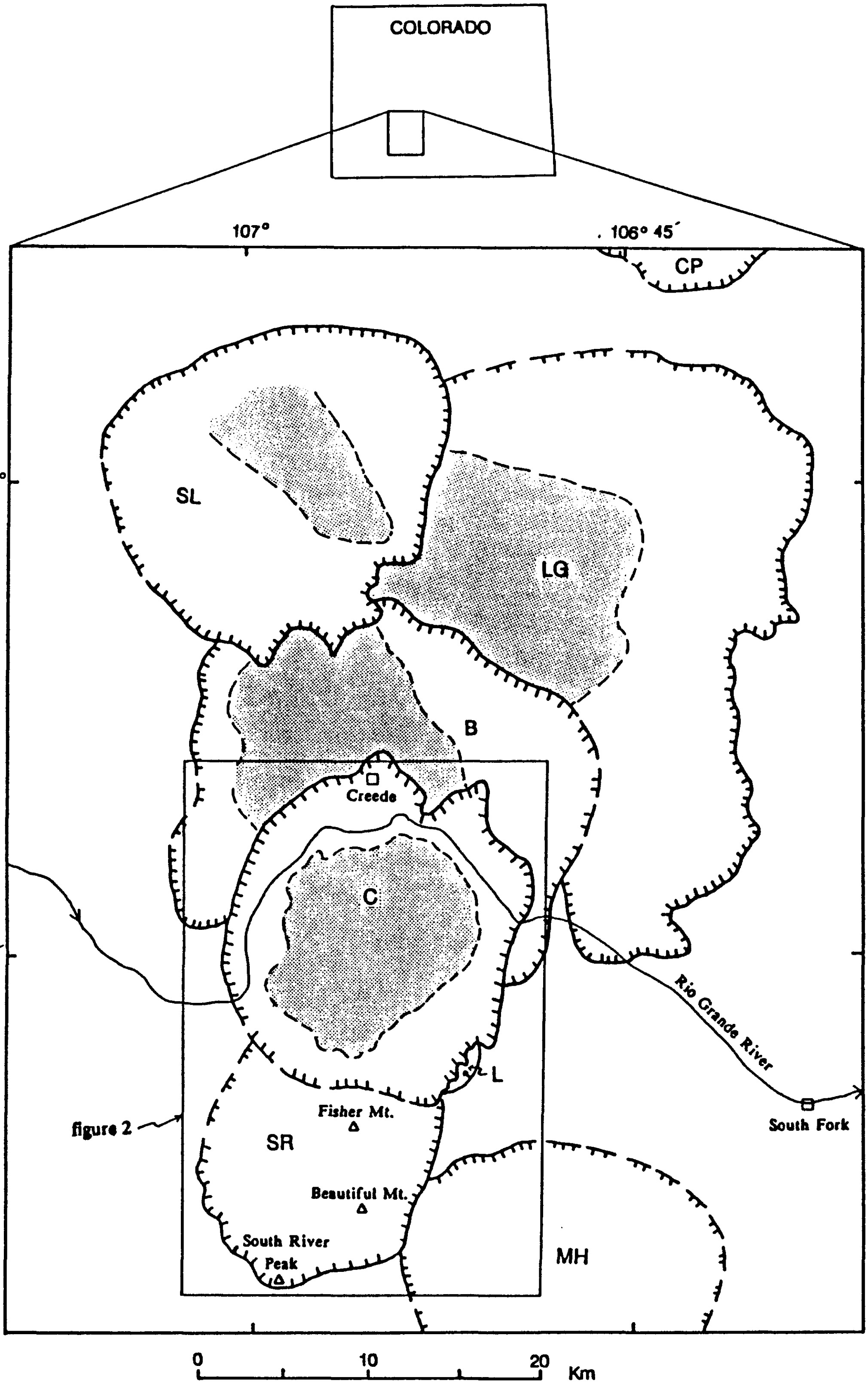

Figure 1. Map of the central San Juan caldera cluster showing location of geologic map included in (fig. 2) and selected geographic features. Caldera margins are shown by hachured lines, stipple pattern shows intra-caldera resurgent uplifts. Bar and ball symbol is on downdropped side of a ring fault related to Lake Humphreys caldera eruption. Key to calderas: B, Bachelor; C, Creede; CP, Cochetopa Park; LG, La Garita; L, Lake Humphreys; MH, Mount Hope; SL, San Luis; SR, South River. Modified after Lipman and others (1989 figure 3.2).

The 84 new major-oxide and trace-element chemical analyses (tables 2 and 3 respectively) are mainly for post-collapse andesitic (53-63% SiO_2) and dacitic (63-70% SiO_2) lava flows, mudflow deposits, and intrusions related to the South River and Creede calderas. Table 4 provides rock type and sample locality information, and table 5 contains mineralogic data. Geochemical sampling was done while mapping the geology at 1:24,000- scale during the summers of 1986-1989. Previously published mapping in this region is at 1:250,000- and 1:62,500- scales (Steven and Lipman, 1973; Steven and others, 1974). Previous petrologic studies on andesites of this region have been done by Askren and others (1988, 1989). A combined geologic and sample locality map at 1:50,000 scale (fig. 2) provides a context for the chemical data (tables 2 and 3). The chemical data are also compiled on a 5 1/4" floppy disc in spreadsheet format and are included with this report. This file may be accessed by any program which accepts spreadsheet files in the *.WK1 format. Petrographic descriptions and chemical data compilation are by Yager; geologic interpretation is by Lipman and Sawyer.

Much of the study area is relatively remote and rugged, and includes parts of the Rio Grande National Forest and the Weminuche Wilderness. Topographic relief ranges from 2,653 meters elevation near the town of Creede, Colorado, to 4,008 meters on the Continental Divide at South River Peak. Although established trails near Ivy, Fisher, and Goose Creeks (fig. 2) provided access to the remote areas near South River Peak, back-country camps were necessary to permit detailed geologic mapping and sampling.

GEOLOGIC SETTING

Igneous activity began in the San Juan volcanic field at about 35 Ma with eruption of intermediate-composition lava flows and breccias of the Conejos Formation. These eruptions continued until 30 Ma when large caldera-forming eruptions of ash flows began. Andesitic to rhyolitic lava flows erupted intermittently between the caldera-forming eruptions, from vents commonly localized by caldera structures (table 1; fig. 2). Bimodal volcanism (basalt and rhyolite) began at about 26 Ma and continued to 5 Ma, coincident with opening of the Rio Grande rift (Lipman and others, 1970).

Eight major caldera-forming eruptions in the central San Juans (table 1) occurred 28.3 Ma - 26.1 Ma (Steven and Ratté, 1965; Steven and Lipman, 1976; Lanphere, 1988; Lipman and others, 1989). Voluminous post-collapse lavas along the south side of the central caldera cluster were previously mapped entirely as Fisher Quartz Latite and interpreted as Creede caldera-fill (Steven and Lipman, 1973, 1976; Steven and others, 1974). These rocks are now interpreted to be separable and related to formation of at least two calderas in the southern part of the cluster: the volcanic rocks of South River Peak are spatially related to the recently recognized South River caldera that erupted the Wason Park Tuff at 27.2 Ma, and the Fisher Quartz Latite, related to the Creede caldera that erupted Snowshoe Mountain Tuff at 26.9 Ma, Lipman and others (1989).

The newly identified Lake Humphreys caldera, is the source of the tuff of Blue Creek, a discrete ash-flow sheet only recently recognized as separate from the dacitic upper part (Mammoth Mountain member) of the Carpenter Ridge Tuff (Lipman and Sawyer, 1988). Evidence for existence of the Lake Humphreys caldera includes the intracaldera character of the tuff of Blue Creek in the Lake Humphreys area, and preservation of an arcuate ring fault that drops the thick intracaldera tuff of Blue Creek down against early intermediate-composition lavas and breccias of the Conejos Formation. The tuff of Blue Creek near Lake Humphreys has several characteristics of an intracaldera assemblage: exceptional thickness (several hundred meters, with no base exposed), dense welding, and propylitic alteration. Younger dacitic lava flows (Fisher Quartz Latite) unconformably overlie both the intracaldera tuff of Blue Creek, rocks of the Conejos Formation, and the ring fault near Lake Humphreys. The earliest lava flows in the study area, the volcanics of Table Mountain, may represent postcaldera volcanism related to the Lake Humphreys caldera, or alternatively incipient volcanism related to development of the South River caldera.

CALDERA-RELATED LAVA FLOWS

Volcanics of Table Mountain

The volcanics of Table Mountain (Ttm) overlie the tuff of Blue Creek, previously included in the Mammoth Mountain member of the Carpenter Ridge Tuff, and also predate the Wason Park Tuff (fig. 3) (Steven and Lipman, 1973). The volcanics of Table Mountain include lava flows, mudflow deposits, and small intrusions of fine-grained andesite and porphyritic dacite (59-68% SiO_2). Dominant phenocrysts are plagioclase and hornblende; some flows also contain pyroxene or biotite.

The volcanics of Table Mountain are chemically distinct from post-collapse lavas related to both the South River and Creede calderas. The Table Mountain lavas have lower potassium concentrations relative to total iron

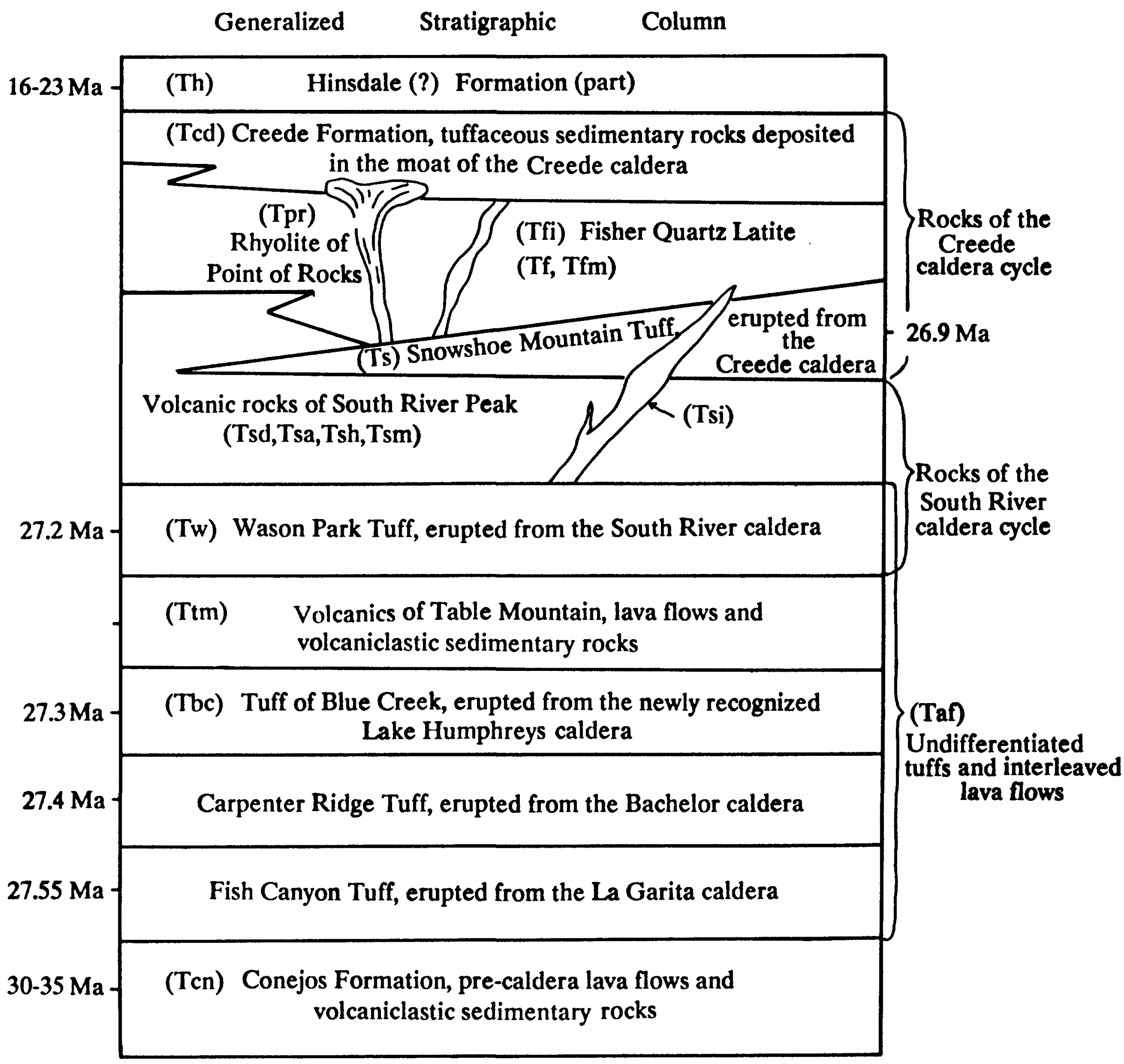

Figure 3. Generalized stratigraphic column of rocks in the south-central San Juan Mountains. Modified from Lanphere, 1988; Lipman and Sawyer, 1988; Lipman and others, 1989; and Marvin Lanphere unpublished data, 1990. Refer to figure 2 for more detailed descriptions of all units except Taf volcanics. Description of Taf may be found in Steven and others (1974), and Lipman and others (1989). Letter symbols in parentheses correspond to those used on geologic map (figure 2).

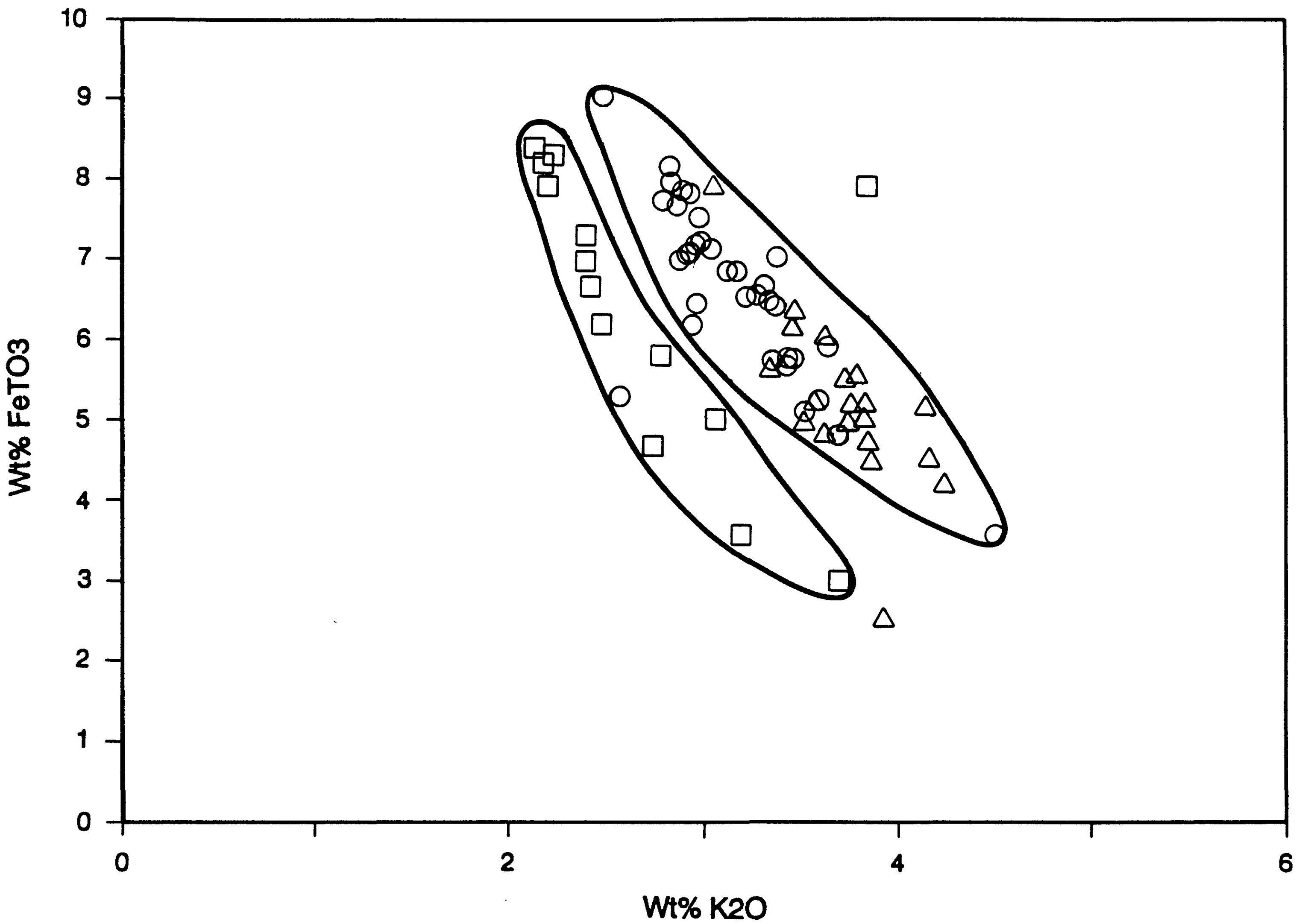

Figure 4. Total iron versus potassium plot for the volcanic rocks of Table Mountain (squares) and the post-collapse lava flows of the South River (circles) and Creede (triangles) calderas. Field boundaries are shown as solid lines around the volcanics of Table Mountain, and the combined South River and Creede post-collapse lava flows.

The volcanic rocks of South River Peak and volcanics of Table Mountain samples that plot outside field boundaries are possibly due to alteration. Chemical distinctions between the Table Mountain and younger post-collapse lavas are also seen in variation diagrams of rubidium versus strontium as well as potassium versus silica and titanium versus silica.

The volcanics of Table Mountain are tentatively interpreted as representing post-caldera volcanism related to the Lake Humphreys caldera, based on their stratigraphic position above the tuff of Blue Creek east of Table Mountain, and their areal distribution proximal to the Lake Humphreys caldera. Alternatively, the volcanics of Table Mountain could constitute incipient volcanism related to development of the South River caldera. A third possibility is that the volcanics of Table Mountain record extracaldera volcanism, unrelated to any caldera. In addition to the volcanics of Table Mountain, unnamed lava flows between the tuff of Blue Creek and the Wason Park Tuff exposed in lower Goose Creek and Wagon Wheel Gap may also be part of post-collapse volcanism related to the Lake Humphreys caldera.

Volcanic rocks of South River Peak

The South River caldera, associated with eruption of the Wason Park Tuff, is largely filled by andesitic to mafic dacitic lava and mudflow deposits, here designated the volcanic rocks of South River Peak. The base of the intracaldera lavas is not exposed, but they are at least 900 meters thick. Additional evidence for the South River caldera includes the dense welding of outflow Wason Park Tuff beyond the South River caldera, and contact relations at the South River caldera topographic wall. Lava flows within the caldera, belonging to the volcanic rocks of South River Peak, lap against the older Carpenter Ridge Tuff, tuff of Blue Creek, and Wason Park Tuff along a steep unconformity that defines the topographic wall of the South River caldera for almost 180^{o} of arc, from upper Red Mountain Creek eastward, along the Continental Divide, and into upper Goose Creek (fig. 2).

The volcanic rocks of South River Peak contain three dominant lithologies: 1) andesite, 2) hornblende andesite, and 3) mafic dacite (fig. 3). All lithologies are finely porphyritic and contain plagioclase averaging 2.5 mm in length.

The andesite unit consists of dark-gray, fine-grained lava flows, exposed mainly low in the stratigraphic sequence of the volcanic rocks of South River Peak along the southern margin of the South River caldera. These flows range from 56-61% in SiO_2 content and contain phenocrysts of plagioclase, clinopyroxene, +/- orthopyroxene, +/- sparse hornblende, and iron-titanium oxides.

Hornblende andesite is more silicic (59-62% SiO_2), mostly lighter in color, and more coarsely porphyritic than andesite. It contains more abundant and larger hornblende phenocrysts; hornblende predominates over pyroxene as the dominant mafic mineral, and some flows also contain sparse biotite.

The mafic dacite flows crop out on Beautiful Mountain (fig. 1) and in Fisher Creek. They mostly occur high in the stratigraphic sequence of the volcanic rocks of South River Peak and are compositionally transitional into the overlying dacite of the Fisher Quartz Latite. Mafic dacite mostly ranges from 62-63% SiO_2, although a few andesite, as well as more silicic dacite, lava flows are interbedded in this unit. The phenocryst mineralogy of the mafic dacites is similar to the hornblende andesites, except that biotite is common.

In contrast with other calderas of the central San Juan cluster, there was no post-collapse resurgence of the South River caldera. Except for the andesite (56-62% SiO_2) and mafic dacite (62-63% SiO_2) along the southern margin, the South River caldera probably remained incompletely filled until after the Creede caldera formed. After eruption of the Snowshoe Mountain Tuff, post-collapse dacite lavas of the Fisher Quartz Latite (Tf; mostly 63-68% SiO_2), filled the northern parts of the South River caldera.

Although lava flows of the volcanic rocks of South River Peak were erupted from vents along the south margin of the South River caldera and are dominantly more mafic than younger lava flows of the Fisher Quartz Latite, stratigraphic and petrologic relations among these two lava types are locally complex. Lava flows of the volcanic rocks of South River Peak mostly dip toward the northeast from South River Peak, inward toward the center of the caldera, and mostly underlie the more silicic lava flows of the Fisher Quartz Latite and breccias related to the Creede caldera. Nevertheless, silicic dacite is locally present low in the sequence of the volcanic rocks of South River Peak, and fine-grained andesite continued to be erupted within the South River caldera area (near South River Peak) after formation of the Creede caldera. Silicic dacite lavas similar to the Fisher Quartz Latite are locally present low in the Fisher and Ivy Creek drainages (fig. 2), and clasts of silicic dacite (>63% SiO_2) in mudflow deposits low in the South River Peak assemblage also document eruption of relatively evolved Fisher Quartz Latite-type magma early during the South River caldera cycle. Conversely, outflow facies Snowshoe Mountain Tuff near the south margin of the South River caldera (along the Continental Divide) is cut by an andesite dike and overlain by several andesite lavas and interbedded mudflow deposits, providing evidence for the continued presence of andesite magma beneath the South River caldera during the Creede caldera cycle.

Volcanic rocks on Beautiful Mountain (fig. 2) are chemically and petrographically transitional between the volcanic rocks of South River Peak and Fisher Quartz Latite. In general, Beautiful Mountain rocks show intermediate concentrations of rubidium with respect to strontium and are transitional to concentrations seen in Fisher Quartz Latite (fig. 5). Also, strontium concentrations of Beautiful Mountain rocks have a similar range to those in Fisher Quartz Latite (fig. 5). These rocks are included in the volcanic rocks of South River Peak because (1) texturally they are similar, and (2) in the Beautiful Mountain area they underlie more coarsely porphyritic lavas typical of Fisher Quartz Latite.

Intrusions of andesite and fine-grained diorite (Tsi) occur west and southwest of South River Peak and near Goose Creek. The intrusive rocks include fine-grained, dark-gray dikes and larger irregular bodies of variable texture that are interpreted as near-roof-level exposures of an arcuate ring intrusion along the south margin of the South River caldera. These intrusions may be related to the South River caldera cycle, as indicated by local cross-cutting relations with the Wason Park Tuff, by their distribution along the southwestern to southeastern margins of the South River caldera, and by associated hydrothermal alteration that extends into the volcanic rocks of South River Peak. The intrusive rocks are likely to be feeders for the volcanic rocks of South River Peak, because of their similar mineralogy and chemistry. Larger intrusions near South River Peak and Goose Creek, and adjacent wall rocks, are variably propylitically altered, silicified, and pyritized.

Fisher Quartz Latite

The topographic margins of the South River and younger Creede calderas overlap near Fisher Mountain (fig.2), where they are buried by a 0.6-km-thick section of silicic dacite, previously mapped and named as Fisher Quartz Latite. These lavas are inferred to have erupted along the ring fractures of the South River and Creede calderas. Fisher Quartz Latite magmatism commenced after eruption of the Snowshoe Mountain Tuff; a few Fisher Quartz Latite lava flows are domed by Creede caldera resurgence, and lava eruptions continued during deposition of volcaniclastic lake sediments (Creede Formation, in the topographic moat of the Creede caldera). Some Fisher Quartz Latite lava flows are as much as several hundred meters thick, where they ponded in the Creede caldera moat or against the topographic wall of the caldera. The Creede caldera is strongly domed, and eruption of the Fisher Quartz Latite may have been associated with magmatic resurgence of the caldera.

The Fisher Quartz Latite is generally more silicic and more coarsely porphyritic than the volcanic rocks of South River Peak. Although dacites are volumetrically dominant, analyses of Fisher Quartz Latite lava flows vary from 59-73% SiO_2, averaging ~64.4% and including two andesite samples and one rhyolite sample. Phenocrysts include plagioclase (averaging 3.5 mm long), hornblende, biotite, iron-titanium oxides, +/- pyroxene, +/- sanidine (locally up to 4 cm and resorbed), +/- trace sphene, and +/- trace quartz.

Subtle chemical differences exist, especially in trace elements, between the volcanic rocks of South River Peak and the Fisher Quartz Latite, in addition to the more silicic average compositions of the latter. Fisher Quartz Latite generally has higher rubidium versus strontium than do the volcanic rocks of South River Peak (fig. 5), although, there is overlap for the transitional Beautiful Mountain lava flows. One mudflow clast in the volcanic rocks of South River Peak has a similar rubidium concentration to that seen in the Fisher Quartz Latite.

Volcanics of Point of Rocks

The volcanics of Point of Rocks consist of light-gray, flow-laminated, high-silica rhyolite (75% SiO_2) that occur as erosional remnants of a small lava dome complex on the northwestern margin of the Creede caldera resurgent dome (Steven and Ratté, 1973). Phenocrysts include sanidine, plagioclase, biotite, and traces of quartz. Rare-earth-element data show this unit to be transitional to the bimodal basalt - rhyolite episode of volcanism (Hinsdale Formation) in the San Juan volcanic field (Lipman, 1987).

HINSDALE FORMATION (?)

Lava flows of xenocrystic basalt to dacite are probably correlative with the regionally distributed Hinsdale Formation, and are the youngest volcanic unit in the study area, overlying lava flows of the Fisher Quartz Latite along the ridge northeast of Beautiful Mountain (fig. 2). These lava flows contain small sparse phenocrysts of plagioclase, augite, and oxidized hornblende; xenocrysts of resorbed quartz are distinctive. None of the older caldera-related lava flows contain resorbed quartz.

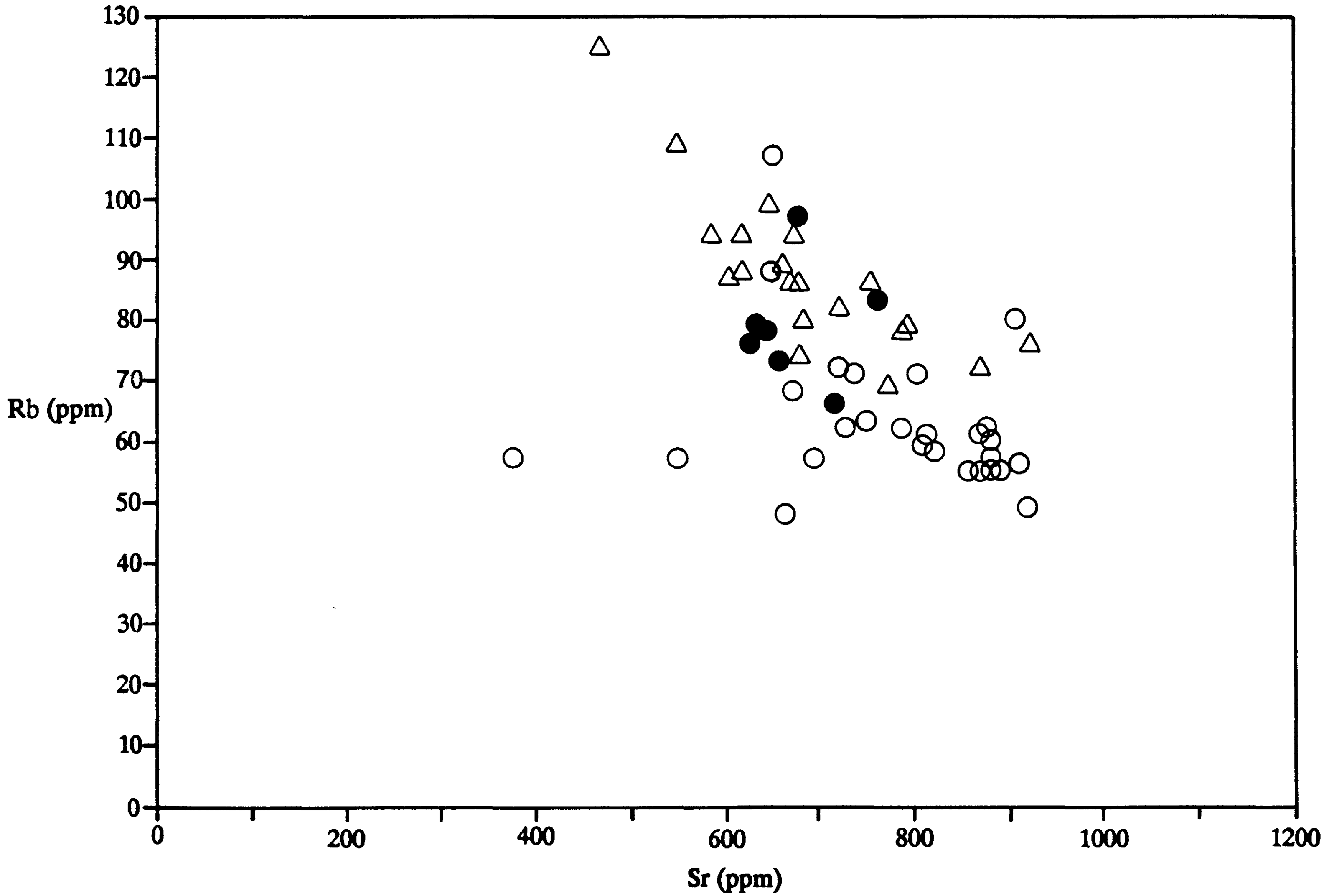

Figure 5. Rubidium versus strontium trace element variation diagram (in parts per million) comparing the post-collapse lava flows of the South River (circles) and Creede (triangles) calderas. Filled circles are rocks occurring on and or near Beautiful Mountain (fig.2).

CHEMICAL CLASSIFICATION OF THE VOLCANIC ROCKS OF SOUTH RIVER PEAK AND FISHER QUARTZ LATITE

Based on the IUGS total alkali-silica classification of Le Bas and others, (1986), most volcanic rocks of South River Peak plot in the trachyandesite field, whereas most Fisher Quartz Latite samples plot as trachydacites (fig. 6). The most mafic Fisher Quartz Latite lava flows contain resorbed sanidine. Some volcanic rocks of South River Peak are compositionally transitional into the Fisher Quartz Latite lava flows, especially the samples from Beautiful Mountain, as noted previously. Although all these lava flows have alkaline affinities, they lack alkaline phenocryst minerals such as sodic pyroxenes or amphiboles. Alternatively, based on the alkaline/sub-alkaline classification of Irvine and Baragar (1971), all of the South River Peak and Fisher Quartz Latite lava flows are subalkaline (fig. 6).

ANALYTICAL METHODS

Wavelength dispersive X-ray fluorescence analyses (major oxides) were made at the U.S. Geological Survey, Branch of Geochemistry in Denver. Energy dispersive X-ray fluorescence (EDXRF) trace-element analyses were made using the methods of Elsass and DuBray (1982) and of Quick and Haleby (1988). The two EDXRF methods are comparable (J. Quick and D. Yager, unpublished data, 1988), and analytical precision of the Elsass and duBray EDXRF technique is discussed in Sawyer and Sargent (1989).

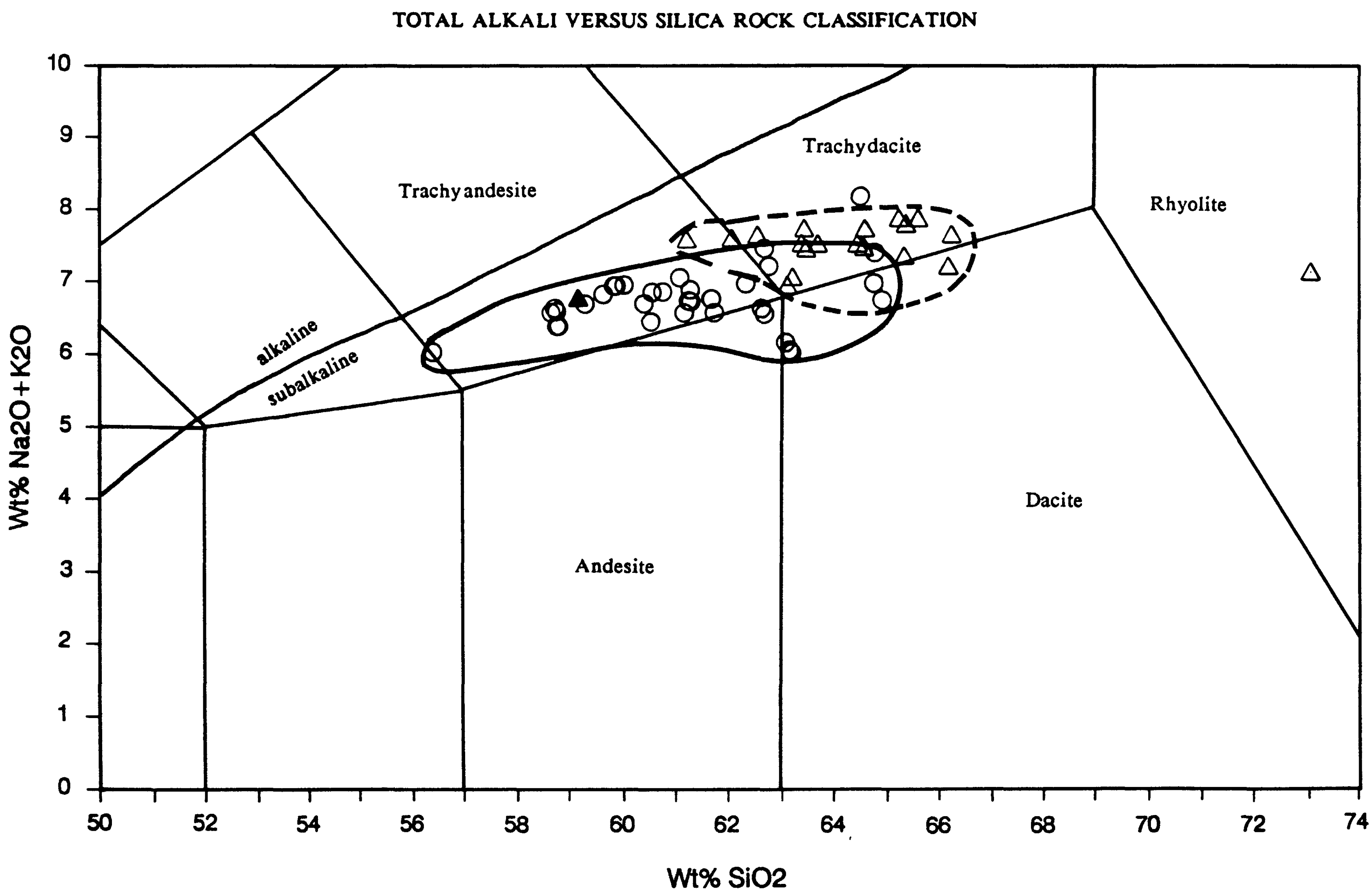

Figure 6. Total alkali versus silica plot showing distinctions between volcanic rocks of South River Peak (circles) and Fisher Quartz Latite (triangles). Rock classification fields shown are after Le Bas and others (1986). The alkaline-subalkaline distinction of Irvine and others (1971) is also shown. The solid triangle is the most mafic Fisher Quartz Latite sample, and contains resorbed sanidine.

ACKNOWLEDGEMENTS

We thank Jim Basham and Jerry Dennis of Creede, Colorado for their back-country camp support. Wavelength dispersive x-ray fluorescence analyses by J. Taggart, A. Bartel, and D. Siems are greatly appreciated.

REFERENCES CITED

Askren, D.R., Roden, M.F., and Whitney, J.A., 1988, Origin and implications of small-volume andesites interlayered with large-volume ash-flow tuffs of the San Juan volcanic field, south central Colorado (abs.): Geological Society of America Centennial Celebration Abstracts with Programs, v. 20, no.7, p. A369.

_______ 1989, Small volume andesites interlayered with large volume ash-flow tuffs in the San Juan (CO), Indian Peak (UT-NV), and Central Nevada volcanic complexes (abs.): International Association of Volcanology and Chemistry of the Earth's Interior, Continental Magmatism Abstracts, New Mexico Bureau of Mines Bulletin 131, p. 9.

Elsass, F.E., and du Bray, E.A., 1982, Energy-dispersive X-ray fluorescence spectrometry using the KEVEX 7000 system: Saudi Arabian Deputy Ministry for Mineral Resources Open-File Report USGS-OF-02-52, 53 p.

Irvine, T.N. and Baragar, R.A., 1971, A Guide to the Chemical Classification of Igneous Rocks: Canadian Journal of Earth Sciences,
v. 8, p.523-548.

Lanphere, M.A., 1988, High resolution $^{40}Ar/^{39}Ar$ chronology of Oligocene volcanic rocks, San Juan Mountains, Colorado: Geochemica et Cosmica Acta, v. 52, p. 1425-1434.

Le Bas, M.J., Le Maitre, R.W., Streckeisen, A., and Zanettin, B., 1986, A Chemical Classification of Volcanic Rocks Based on The Total Alkali-Silica Diagram: Journal of Petrology, v. 27, p. 745-750.

Lipman, P.W., 1987, Rare-earth-element compositions of Cenozoic volcanic rocks in the southern Rocky Mountains and adjacent areas: U.S. Geological Survey Bulletin 1668, 23 p.

Lipman, P.W., Steven, T.A., and Mehnert, H.H., 1970, Volcanic areas: history of the San Juan Mountains, Colorado, as indicated by potassium-argon dating: Geological Society of America Bulletin, v. 81, p. 2329-2352.

Lipman, P.W., and Sawyer, D.A., 1988, Preliminary geology of the San Luis Peak Quadrangle and adjacent areas, San Juan Volcanic Field, Southwestern Colorado: U.S. Geological Survey Open-File Report 88-359, 32 p.

Lipman, P.W., Sawyer, D.A., and Hon, K., 1989, Excursion 16B: Oligocene-Miocene San Juan volcanic field, Colorado, in Chapin, C.E., and Zidek, J., eds., Field excursions to volcanic terranes in the western United States, Volume I: Southern Rocky Mountain region: New Mexico Bureau of Mines and Mineral Resources Memoir 46, p. 330-350.

Quick, J.E., and Haleby, A.M., 1988, XAP, a program for deconvolution and analysis of complex x-ray spectra: Saudi Arabian Ministry of Petroleum and Mineral Resources, Technical Record, USGS-TR-O8-3, 33 p.

Ratté, J.C., and Steven, T.A., 1967, Ash flows and related volcanic rocks associated with the Creede caldera, San Juan Mountains, Colorado: U.S. Geological Survey Professional Paper 524-H, p. H1-H57.

Sawyer, D.A., and Sargent K.A., 1989, Petrologic evolution of divergent peralkaline magmas from the Silent Canyon caldera complex, southwestern Nevada volcanic field: Journal of Geophysical Research, v. 94, no. B5, p. 6021-6040.

Steven, T.A., and Ratté, J.C., 1965, Geology and structural control of ore deposition in the Creede district, San Juan Mountains, Colorado: U.S. Geological Survey Professional Paper 475-D, p. D54-D63.

Steven, T.A., and Lipman, P.W., 1973: Geologic map of the Spar City Quadrangle, Mineral County, CO, U.S. Geological Survey Map, GQ-1052. Scale 1:62,500

Steven, T.A., and Ratté, J.C., 1973, Geologic map of the Creede Quadrangle, Mineral and Saguache Counties, CO, U.S. Geological Survey, GQ-1053.

Steven, T.A., and Lipman, P.W., 1976, Calderas of the San Juan volcanic field,southwestern Colorado: U.S. Geological Survey Professional Paper 958, 35 p.

Steven, T.A., Lipman, P.W., Hail, W.J., Jr., Barker, F., and Luedke, R.G., 1974, Geologic Map of the Durango Quadrangle, Southwestern Colorado: U.S. Geological Survey Miscellaneous Investigation Series Map, I-764. Scale 1:250,000

Table 2. Major-oxide data (calculated volatile free) for volcanic rocks discussed in this report. Sample numbers correspond to localities in figure 2. Major-oxide analysis were done at the U.S. Geological Survey in Denver by analysts J. Taggart, A. Bartel, and D. Siems.

Field No.	Formation Map Symbol	%SIO2	%AL2O3	FETO3	%MGO	%CAO	%NA2O	%K2O	%TIO2	%P2O5	%MNO	LOI	oxide sum + LOI
88L-67	Th?	58.8	15.36	8.44	2.66	6.25	3.68	2.49	1.23	0.45	0.11	1.06	99.50
88L-68	Th?	57.9	15.39	8.65	3.60	6.11	3.66	2.43	1.25	0.46	0.12	0.56	99.60
88L-69	Th?	61.4	14.71	7.24	2.51	5.56	3.60	3.21	1.03	0.41	0.11	0.77	99.76
89L-100	Th?	60.4	14.45	7.35	3.05	5.85	3.55	3.15	1.05	0.42	0.10	1.06	99.43
89L-118	Th?	63.6	14.11	6.27	2.30	4.92	3.62	3.35	0.89	0.34	0.09	0.77	99.47
TPR-3	Tpr	75.12	13.78	0.92	0.17	0.46	3.03	5.62	0.19	0.00	0.00	1.06	99.30
85L-39	Tf	65.4	15.41	5.01	1.66	4.07	3.46	3.85	0.66	0.27	0.07	1.93	99.84
SJ85-47	Tf	73.1	13.84	2.52	0.84	2.19	3.26	3.93	0.47	0.09	0.00	1.23	100.25
89L-101	Tf	61.2	15.86	6.35	2.32	4.72	4.10	3.48	0.94	0.47	0.05	1.01	99.52
89L-102	Tf	63.2	15.72	5.50	2.31	4.50	3.16	3.75	0.66	0.31	0.08	2.63	99.16
89L-107	Tf	66.2	15.20	4.98	1.31	3.67	3.62	3.54	0.54	0.23	0.05	0.67	99.41
89L-112	Tf	63.6	15.71	5.55	2.08	4.00	3.62	3.81	0.66	0.31	0.06	0.72	99.36
89L-120	Tf	64.7	15.57	4.73	1.76	3.77	3.84	3.86	0.61	0.28	0.08	1.69	99.20
DY89-6	Tf	64.5	15.60	5.18	1.84	3.96	3.72	3.78	0.67	0.30	0.09	1.29	99.68
DY89-10	Tf	65.3	15.68	5.19	1.17	3.57	3.98	3.85	0.64	0.29	0.08	0.52	99.79
DY89-11A	Tf	63.4	16.47	4.82	1.59	4.25	3.86	3.64	0.63	0.34	0.10	1.61	99.12
DY89-11B	Tf	59.2	16.44	7.90	2.11	5.54	3.66	3.07	0.97	0.39	0.12	0.86	99.41
DY89-12	Tf	62.6	16.26	6.01	1.33	4.18	3.96	3.64	0.83	0.37	0.11	0.98	99.31
DY89-14	Tf	65.7	15.32	4.51	1.73	3.55	3.67	4.18	0.61	0.29	0.08	2.06	99.59
DS89001	Tf	63.8	16.07	4.95	1.75	4.32	3.72	3.76	0.66	0.35	0.10	1.68	99.47
DS89003	Tf	65.5	15.71	4.48	1.69	3.58	3.89	3.88	0.57	0.27	0.08	1.97	99.64
DS89004	Tf	66.3	16.41	4.20	1.14	2.85	3.34	4.25	0.63	0.12	0.03	1.25	99.31
DS89006	Tfm	64.7	15.60	5.15	1.88	4.16	3.29	4.15	0.63	0.33	0.09	1.95	99.95
DS89012	Tf	63.5	16.71	5.22	1.08	4.46	4.12	3.58	0.68	0.36	0.10	0.64	99.82
DS89014	Tf	62.1	16.68	6.14	1.13	4.56	4.08	3.48	0.78	0.41	0.07	1.10	99.42
DS89015	Tf	63.3	16.16	5.61	2.10	4.54	3.65	3.36	0.67	0.34	0.07	2.21	99.81
DS89028	Tsd	65.0	16.19	4.81	1.72	4.64	3.01	3.72	0.48	0.23	0.09	2.40	99.85
DY89-7	Tsd	62.7	15.93	5.90	1.96	4.31	3.79	3.65	0.73	0.34	0.18	0.80	99.49
DY89-8	Tsd	62.4	15.57	6.48	2.35	4.90	3.59	3.35	0.77	0.34	0.11	0.42	99.82
DY89-9	Tsd	62.8	15.90	5.77	2.03	4.57	3.74	3.45	0.70	0.37	0.11	1.24	99.42
DS89016	Tsd	64.9	15.63	5.23	1.26	4.04	3.78	3.60	0.63	0.32	0.12	0.80	99.53
DS89017	Tsa	59.9	16.42	7.08	2.07	5.45	3.96	2.95	0.87	0.47	0.09	0.70	99.28

Table 2 continued.

Field No.	Formation Map Symbol	%SIO2	%AL2O3	FETO3	%MGO	%CAO	%NA2O	%K2O	%TIO2	%P2O5	%MNO	LOI	oxide sum + LOI
DS89019	Tsh	59.3	16.32	7.86	2.14	5.78	3.75	2.91	0.96	0.48	0.12	0.72	99.64
DS89029	Tsh	60.6	15.70	6.98	2.89	5.53	3.53	2.89	0.79	0.31	0.11	1.27	99.30
DS89030	Tsh	61.1	15.40	5.74	1.62	8.01	3.65	3.37	0.69	0.30	0.09	3.26	99.97
DS89034	Tsd	64.8	15.36	5.10	1.96	4.14	3.41	3.53	0.59	0.24	0.08	1.70	99.23
DS89035	Tsd	62.6	16.02	6.52	2.24	4.68	3.37	3.23	0.77	0.27	0.09	1.99	99.84
88L-32	Tsi	61.4	16.95	6.38	1.95	5.42	3.32	3.05	0.74	0.40	0.17	3.81	99.81
88L-34	Tsi	57.6	17.56	7.30	2.40	6.59	3.94	2.63	0.84	0.55	0.17	1.47	99.52
88L-36	Tsi	58.3	17.37	7.77	2.36	5.80	4.11	2.35	0.82	0.52	0.15	1.55	99.56
88L-61	Tsi	59.0	16.83	7.63	2.42	5.68	3.87	2.70	0.83	0.47	0.13	1.34	99.55
89L-129	Tsi	53.8	17.84	9.70	2.32	8.37	3.45	2.09	1.32	0.76	0.13	1.35	99.81
88L-31A	Tsa	56.4	16.42	9.03	3.32	6.59	3.51	2.49	1.14	0.51	0.12	0.72	99.53
88L-31B	Tsa	60.6	18.46	7.02	0.71	4.93	3.45	3.39	0.77	0.42	0.05	1.41	99.75
88L-31C	Tsh	61.2	17.19	6.43	1.86	5.49	3.58	2.97	0.66	0.38	0.11	1.10	99.85
88L-58	Tsd	63.2	17.45	5.29	1.38	5.23	3.40	2.58	0.60	0.34	0.12	2.59	99.62
88L-62A	Tsh	58.8	16.01	8.15	2.98	5.91	3.53	2.83	0.97	0.44	0.13	1.29	99.69
88L-62B	Tsh	61.8	15.95	7.12	2.37	4.82	3.49	3.05	0.87	0.34	0.16	1.54	99.92
88L-62C	Tsd	63.1	16.01	6.18	2.40	4.73	3.17	2.95	0.72	0.29	0.08	3.82	99.66
88L-62D	Tsd	63.2	15.93	6.86	2.59	4.04	2.89	3.12	0.77	0.33	0.12	5.18	99.82
88L-62E	Tsd	64.5	16.72	3.58	1.12	4.22	3.64	4.51	0.75	0.23	0.04	1.92	99.37
88L-65	Tsh	58.7	16.34	7.73	2.79	5.89	3.77	2.79	0.93	0.50	0.16	0.88	99.64
88L-66	Tsh	61.3	16.24	6.40	2.34	5.11	3.32	3.38	0.79	0.45	0.10	2.06	99.39
88L-70	Tsh	59.7	16.43	7.51	2.10	5.53	3.81	2.98	0.93	0.49	0.10	0.76	99.53
89L-115	Tsh	60.8	16.31	6.84	2.35	5.17	3.65	3.18	0.80	0.43	0.12	1.29	99.63
89L-122	Tsh	58.7	16.25	7.85	2.67	5.80	3.74	2.87	0.97	0.48	0.12	0.89	99.48
89L-123	Tsd	62.7	15.71	5.74	2.29	4.46	3.97	3.48	0.72	0.36	0.10	1.95	99.56
89L-128	Tsm	61.7	17.48	5.67	1.76	5.49	3.29	3.44	0.59	0.40	0.11	1.58	99.90
89L-130	Tsm	62.7	16.58	6.57	1.84	4.34	3.25	3.27	0.70	0.26	0.15	2.27	99.69
89L-135A	Tsi	57.8	17.26	8.24	2.53	6.52	3.46	2.31	0.91	0.48	0.16	0.34	99.67
89L-135B	Tsi	63.0	16.66	5.30	1.56	5.48	3.70	2.44	0.50	0.25	0.13	2.74	99.07
89L-143	Tsi	65.4	16.08	5.04	1.76	4.07	3.44	2.65	0.49	0.22	0.16	2.35	99.36
89L-144	Tsi	63.2	16.62	5.22	1.88	5.24	3.43	2.69	0.49	0.25	0.31	2.50	99.31
DY89-16	Tsh	58.8	16.56	7.94	2.44	5.68	3.53	2.84	1.00	0.51	0.10	1.54	99.41

Table 2 continued.

Field No.	Formation Map Symbol	%SIO2	%AL2O3	FETO3	%MGO	%CAO	%NA2O	%K2O	%TIO2	%P2O5	%MNO	LOI	oxide sum + LOI
DY89-17	Tsa	60.1	16.33	7.21	2.21	5.52	3.93	2.99	0.90	0.49	0.10	0.77	99.74
DY89-18	Tsh	58.7	16.27	7.81	2.74	5.83	3.62	2.94	0.97	0.50	0.12	1.04	99.51
DS89007	Tsh	60.4	16.46	7.18	2.22	5.15	3.70	2.97	0.85	0.46	0.13	2.15	99.52
DS89008	Tsh	61.3	16.21	6.67	2.22	5.09	3.54	3.32	0.79	0.44	0.11	1.30	99.68
DS89009	Tsh	58.8	16.25	7.66	2.69	5.74	3.69	2.87	0.94	0.48	0.14	0.29	99.23
DS89010	Tsa	59.8	16.49	7.07	2.36	5.63	3.98	2.93	0.85	0.46	0.10	0.52	99.68
89L-136	Ttm	59.9	17.00	7.30	2.25	6.21	3.27	2.40	0.72	0.33	0.12	1.18	99.51
89L-137	Ttm	64.8	16.01	5.00	1.69	4.58	3.40	3.07	0.48	0.24	0.09	2.57	99.34
89L-138	Tsi	64.6	16.45	4.67	1.49	4.97	3.56	2.74	0.54	0.25	0.08	1.53	99.36
89L-140	Ttm	67.9	16.53	3.00	0.61	3.36	3.67	3.71	0.32	0.14	0.11	2.59	99.31
89L-141	Ttm	67.4	15.81	3.56	1.05	3.84	3.75	3.20	0.38	0.18	0.05	0.66	99.27
89L-147B	Tsi	59.5	16.07	7.90	3.02	5.18	2.93	3.85	0.95	0.36	0.13	3.52	99.89
DY89-20	Ttm	57.3	17.34	8.39	2.41	6.74	3.72	2.14	0.90	0.49	0.15	0.82	99.55
DY89-21	Ttm	57.5	17.43	8.29	2.53	6.53	3.67	2.24	0.88	0.49	0.16	0.77	99.77
DY89-22	Ttm	60.4	18.51	6.19	1.20	5.97	3.84	2.48	0.68	0.48	0.12	1.12	99.84
DY89-24	Ttm	60.7	17.25	6.98	1.70	5.93	3.61	2.40	0.67	0.33	0.12	0.89	99.74
DY89-24B	Ttm	60.1	17.24	7.91	1.56	5.90	3.63	2.20	0.78	0.40	0.08	1.97	99.78
DY89-25	Ttm	60.8	17.21	6.66	2.13	6.05	3.49	2.43	0.64	0.33	0.15	1.20	99.92
DY89-26	Ttm	58.8	17.26	8.18	2.33	6.35	3.52	2.18	0.77	0.32	0.12	0.90	99.86
DY89-27	Ttm	62.7	17.09	5.80	1.49	5.21	3.65	2.78	0.64	0.33	0.07	1.12	99.76

Table 3. Trace element analyses (in parts per million) for volcanic rocks discussed in this report. Analyses were done at the U.S. Geological Survey by D. Yager. N.A. means data is not available. Sample numbers correspond to localities in figure 2.

Field No.	Formation Map Symbol	%FeO	Zn ppm	Rb ppm	Sr ppm	Y ppm	Zr ppm	Nb ppm	Ba ppm	La ppm	Ce ppm	Nd ppm
88L-67	Th?	7.20	67	49	1119	23	160	10	801	46	94	45
88L-68	Th?	7.50	119	42	1149	24	154	12	864	52	92	56
88L-69	Th?	6.10	106	73	964	24	146	11	896	59	101	58
89L-100	Th?	7.16	114	72	991	24	149	14	851	61	109	52
89L-118	Th?	5.86	113	75	849	22	142	13	791	40	87	34
TPR-3	Tpr	0.70	N.A.	161	68	18	174	21	N.A.	N.A.	N.A.	N.A.
85L-39	Tf	4.40	N.A.	94	587	20	174	21	N.A.	N.A.	N.A.	N.A.
SJ85-47	Tf	3.70	N.A.	125	470	20	145	22	N.A.	N.A.	N.A.	N.A.
89L-101	Tf	6.14	92	76	923	20	211	18	1280	51	92	48
89L-102	Tf	4.81	99	89	663	22	184	14	929	44	72	39
89L-107	Tf	4.60	61	87	607	30	184	13	1043	67	88	59
89L-112	Tf	5.18	106	99	650	27	185	14	1004	47	82	45
89L-120	Tf	4.26	80	86	679	21	160	11	1157	44	77	42
DY89-6	Tf	4.67	107	80	687	22	179	16	1162	47	83	38
DY89-10	Tf	4.79	103	86	672	23	176	14	1180	50	82	38
DY89-11A	Tf	4.44	91	86	756	24	195	14	1237	54	86	45
DY89-11B	Tf	7.97	121	69	776	29	179	14	1098	39	83	44
DY89-12	Tf	5.78	123	79	794	24	196	18	1300	47	92	41
DY89-14	Tf	3.94	83	88	621	24	177	15	1122	49	79	41
DS89001	Tf	4.48	79	82	724	24	174	13	1049	45	73	41
DS89003	Tf	3.92	65	94	675	17	166	14	1169	43	79	37
DS89004	Tf	4.09	86	109	550	20	184	15	951	39	68	42
DS89006	Tfm	4.71	77	94	621	23	187	14	1032	47	88	41
DS89012	Tf	4.93	100	78	791	24	188	14	1230	42	78	41
DS89014	Tf	5.97	91	72	872	25	194	17	1365	55	86	46
DS89015	Tf	5.03	89	74	681	22	186	10	984	44	73	40
DS89028	Tsd	4.40	118	62	730	25	164	10	924	33	62	33
DY89-7	Tsd	5.46	80	97	678	48	196	17	1226	84	98	61
DY89-8	Tsd	6.14	108	78	644	29	181	14	942	42	73	38
DY89-9	Tsd	5.27	103	83	762	27	206	19	1068	41	88	44
DS89016	Tsd	4.79	93	88	650	24	194	15	1041	50	87	44
DS89017	Tsa	6.75	118	56	912	28	208	15	1221	47	86	61

Table 3 continued.

Field No.	Formation Map Symbol	%FeO	Zn ppm	Rb ppm	Sr ppm	Y ppm	Zr ppm	Nb ppm	Ba ppm	La ppm	Ce ppm	Nd ppm
DS89019	Tsh	7.66	122	62	877	29	201	13	1240	47	84	51
DS89029	Tsh	6.72	115	66	716	25	177	14	886	37	69	39
DS89030	Tsh	5.15	111	76	627	29	176	14	928	43	73	37
DS89034	Tsd	4.62	72	79	634	25	181	12	1021	40	73	33
DS89035	Tsd	6.32	109	73	657	27	185	13	951	40	81	43
88L-32	Tsi	5.40	83	54	603	29	204	12	1008	39	80	45
88L-34	Tsi	6.10	139	54	1065	35	206	14	1178	59	98	54
88L-36	Tsi	6.70	116	43	843	30	179	13	959	37	76	52
88L-61	Tsi	6.50	65	59	830	21	175	17	1058	51	80	48
89L-129	Tsi	10.3	158	35	1001	38	153	14	930	43	75	49
88L-31A	Tsa	7.70	112	55	857	24	199	13	905	39	80	44
88L-31B	Tsa	5.80	91	63	749	28	190	12	835	43	73	47
88L-31C	Tsh	5.40	68	57	696	24	187	10	859	41	80	40
88L-58	Tsd	4.30	97	48	664	18	205	11	964	47	78	43
88L-62A	Tsh	7.00	98	59	808	26	185	13	1176	42	88	43
88L-62B	Tsh	5.80	67	68	674	24	186	14	949	40	77	44
88L-62C	Tsd	4.90	66	57	550	16	172	11	974	37	75	42
88L-62D	Tsd	5.60	91	57	376	20	181	8	985	42	71	41
88L-62E	Tsd	3.10	60	72	721	19	180	11	1417	51	82	49
88L-65	Tsh	6.50	121	49	920	25	200	17	1209	50	88	50
88L-66	Tsh	5.30	93	62	788	20	191	16	1561	53	85	47
88L-70	Tsh	6.20	88	60	880	29	216	17	1242	45	87	48
89L-115	Tsh	6.45	93	61	813	29	199	15	1288	49	85	49
89L-122	Tsh	7.77	95	55	896	28	193	16	1206	49	88	44
89L-123	Tsd	5.16	105	80	907	20	181	18	1292	57	94	51
89L-128	Tsm	5.14	117	71	738	33	198	13	1105	46	83	43
89L-130	Tsm	6.38	128	107	652	38	187	13	830	58	101	51
89L-135A	Tsi	8.04	124	47	774	33	210	14	844	44	77	41
89L-135B	Tsi	4.97	95	49	742	22	152	11	865	32	63	29
89L-143	Tsi	4.54	109	47	645	22	136	13	885	36	61	38
89L-144	Tsi	4.91	123	41	673	26	166	10	964	36	64	33
DY89-16	Tsh	7.66	133	55	870	34	192	17	1163	48	86	50

Table 3 continued.

Field No.	Formation Map Symbol	%FeO	Zn ppm	Rb ppm	Sr ppm	Y ppm	Zr ppm	Nb ppm	Ba ppm	La ppm	Ce ppm	Nd ppm
DY89-17	Tsa	7.00	122	61	867	30	212	16	1294	50	91	43
DY89-18	Tsh	7.69	116	57	881	31	204	18	1244	49	89	43
DS89007	Tsh	6.72	126	58	821	30	183	17	1289	49	102	57
DS89008	Tsh	6.12	124	71	804	24	200	15	1288	44	84	44
DS89009	Tsh	7.83	128	55	880	32	189	16	1234	54	88	49
DS89010	Tsa	6.81	99	55	891	25	204	15	1270	52	86	48
89L-136	Ttm	6.88	106	50	703	32	143	11	698	33	64	29
89L-137	Ttm	4.53	89	62	728	21	151	11	967	36	63	35
89L-138	Tsi	4.31	100	48	711	20	129	11	824	36	63	32
89L-140	Ttm	2.73	95	71	539	29	183	14	1043	53	83	44
89L-141	Ttm	3.25	100	56	741	18	159	11	1119	40	67	35
89L-147B	Tsi	7.44	114	80	512	31	165	18	884	38	79	44
DY89-20	Ttm	8.23	132	39	764	35	221	18	837	38	81	38
DY89-21	Ttm	8.17	135	32	762	39	220	13	832	42	81	41
DY89-22	Ttm	5.70	92	46	779	31	193	17	859	36	75	39
DY89-24	Ttm	6.87	112	52	656	30	175	11	792	38	67	37
DY89-24B	Ttm	7.74	126	42	726	29	184	10	764	40	70	39
DY89-25	Ttm	6.11	115	53	661	30	171	10	760	31	62	31
DY89-26	Ttm	7.81	111	39	662	27	153	8	698	36	61	41
DY89-27	Ttm	5.41	68	45	688	26	175	11	916	42	73	35

Table 4. Rock type and general sample locality for volcanic rocks discussed in this report. For precise sample localities, see figure 2.

Field No.	Formation Map Symbol	Rock Type And General Location
88L-67	Th?	xenocrystic andesite flow, on ridge W. above head of
88L-68	Th?	xenocrystic andesite flow, on ridge W. above Ivy Cree
88L-69	Th?	xenocrystic andesite flow, W. above Red Mt. Creek
89L-100	Th?	xenocrystic andesite on ridge between Ivy and Red Mt.
89L-118	Th?	Xenocrystic dacite flow, W. of Ivy Ck.
TPR-3	Tpr	High silica rhyolite, Marshall Park campground
85L-39	Tf	silicic dacite flow, at Wagon Wheel Gap
SJ85-47	Tf	rhyolite flow, McCall Ck.
89L-101	Tf	andesite flow, W. above Ivy Creek
89L-102	Tf	mafic dacite flow, near trail on Ivy Ck.
89L-107	Tf	silicic dacite flow, Lime Creek trail head
89L-112	Tf	dacite flow, Fisher Creek trail
89L-120	Tf	dacite flow, Ivy Ck. trail
DY89-6	Tf	dacite flow, bottom Ivy Ck.
DY89-10	Tf	dacite flow, on trail NE of Goose lake
DY89-11A	Tf	mafic dacite flow, SW of Fisher Mt. summit
DY89-11B	Tf	andesite flow?, SW of Fisher Mt. summit
DY89-12	Tf	mafic dacite flow, summit of Fisher Mt.
DY89-14	Tf	dacite flow, S. of Fisher Mt. summit
DS89001	Tf	mafic dacite flow, W. Palo Alto Ck.
DS89003	Tf	dacite flow, NW on Fisher Mt.
DS89004	Tf	dacite intrusion?, NW on Fisher Mt.
DS89006	Tfm	dacite mudflow clast, W. of Fisher Ck.
DS89012	Tf	mafic dacite flow, N. of Fisher Mt. summit
DS89014	Tf	mafic dacite flow, S. of Fisher Mt. summit
DS89015	Tf	mafic dacite flow, S. of Fisher Mt.
DS89028	Tsd	dacite clast, N. of upper Goose Creek
DY89-7	Tsd	mafic dacite flow, lower Beautiful Mt.
DY89-8	Tsd	mafic dacite flow, summit of Beaut. Mt.
DY89-9	Tsd	mafic dacite flow, SW of summit on Beautiful Mt.
DS89016	Tsd	dacite flow, bottom of Fisher Ck.
DS89017	Tsa	andesite flow, S of Beaut. Mt.
DS89019	Tsh	andesite flow, S of Beaut. Mt.
DS89029	Tsh	andesite flow, E. ridge on Beaut. Mt.
DS89030	Tsh	andesite flow, E. ridge on Beaut. Mt.
DS89034	Tsd	dacite flow, N. Beaut. Mt.
DS89035	Tsd	mafic dacite, N. Beaut. Mt.
88L-32	Tsi	andesite dike, cutting Tmm S. of Piedra Pk.
88L-34	Tsi	andesite intrusion, at head of W. Fk. San Juan R.
88L-36	Tsi	andesite intrusion, on ridge crest NE of Piedra peak
88L-61	Tsi	andesite intrusion, E. of Piedra peak
89L-129	Tsi	andesite dike, E. of SR peak
88L-31A	Tsa	andesite flow, on trail S. of SR peak
88L-31B	Tsa	andesite flow, on trail S. of SR peak
88L-31C	Tsh	andesite flow, on trail S. of SR peak
88L-58	Tsd	mafic dacite flow, capping Piedra Pk.
88L-62A	Tsh	andesite flow, NW of SR peak
88L-62B	Tsh	andesite flow, NW of SR peak
88L-62C	Tsd	mafic dacite flow, NW of SR peak
88L-62D	Tsd	mafic dacite flow, NW of SR peak
88L-62E	Tsd	dacite, (slightly propylitized)
88L-65	Tsh	andesite flow, below SR peak summit
88L-66	Tsh	andesite flow, on ridge S. above head of Ivy Creek
88L-70	Tsh	andesite flow, W. above Red Mt. Creek
89L-115	Tsh	andesite flow, head of Ivy Ck.
89L-122	Tsh	andesite flow, near trail at Goose Lake
89L-123	Tsd	mafic dacite flow at Goose lake
89L-128	Tsm	andesite mudflow clast?, E. of SR peak
89L-130	Tsm	mafic dacite mudflow clast, E. of SR peak
89L-135A	Tsi	andesite intrusion, Sawtooth trail
89L-135B	Tsi	mafic dacite intrusion, upper Goose Ck.
89L-143	Tsi	dacite intrusion, upper Goose Ck.
89L-144	Tsi	mafic dacite intrusion, upper Goose Ck.
DY89-16	Tsh	andesite flow, ridge SE of Goose lake
DY89-17	Tsa	andesite flow, ridge SE of Goose lake
DY89-18	Tsh	andesite flow, N. of Goose Ck
DS89007	Tsh	andesite flow, E. of Goose Lake
DS89008	Tsh	andesite flow, head of Fisher Ck SE of Goose lake
DS89009	Tsh	andesite flow, SE of Goose lake
DS89010	Tsa	andesite flow, SE of Fisher Ck.
89L-136	Ttm	andesite flow, S. of Goose Ck. near cont. divide
89L-137	Ttm	dacite flow, Cont. Divide
89L-138	Tsi	dacite intrusion, W. of Sawtooth Mt., Cont. Divide
89L-140	Ttm	silicic dacite flow, W. of Sawtooth Mt, Cont. Divide
89L-141	Ttm	silicic dacite flow, upper Goose Ck.
89L-147B	Tsi	andesite intrusion, upper Goose Ck.
DY89-20	Ttm	andesite flow, NW of Table Mt.
DY89-21	Ttm	andesite flow, NW of Table Mt.
DY89-22	Ttm	andesite intrusion feeding a flow?, W of Table Mt.
DY89-24	Ttm	andesite flow, NE of Sawtooth Mt. summit
DY89-24B	Ttm	andesite flow, N. of Sawtooth Mt.
DY89-25	Ttm	andesite flow, near base of Sawtooth Mt.
DY89-26	Ttm	andesite flow, NE of Sawtooth Mt.
DY89-27	Ttm	mafic dacite flow?, W. of Sawtooth Mt.

Table 5. Mineralogic data for volcanic rocks discussed in this report. Mineral abbreviations used are as follows: pl=plagioclase, hb=hornblende, bt=biotite, cpx=clinopyroxene, opx=orthopyroxene, px=pyroxene, sn=sanidine, and qtz=quartz.

Field No.	Formation Map Symbol	Mineralogy
88L-67	Th?	hb, cpx, pl, qtz-resorbed, opaques
88L-68	Th?	hb, pl, cpx, qtz-resorbed, opaques
88L-69	Th?	hb-altered, cpx & opx, quartz-embayed, opaques
89L-100	Th?	hb-altered, cpx & opx, qtz-embayed, opaques
89L-118	Th?	hb-altered, cpx & opx, qtz-embayed, opaques
TPR-3	Tpr	pl,bt,sn?,trace qtz
85L-39	Tf	pl, hb, bt, sn, opaques (no thin section)
SJ85-47	Tf	N.A.
89L-101	Tf	pl, hb, cpx & opx, opaques, sphene-trace
89L-102	Tf	pl, hb, bt, opaques
89L-107	Tf	pl, hb, bt, opaques
89L-112	Tf	pl, hb, bt, cpx & opx?, opaques
89L-120	Tf	pl, hb, bt, cpx, opaques
DY89-6	Tf	pl, hb, bt, resorbed sn-trace, opaques
DY89-10	Tf	pl,hb-altered, bt?, opaques, (mafics are altered)
DY89-11A	Tf	pl, hb, bt, opaques
DY89-11B	Tf	pl, hb, bt, cpx, sn-resorbed, opaques, sphene-trace
DY89-12	Tf	pl, hb, bt, cpx, sn-resorbed-trace, sphene, opaques
DY89-14	Tf	pl, hb, bt, cpx & opx, opaques
DS89001	Tf	pl, hb, bt, opaques, sphene-trace
DS89003	Tf	pl, hb, bt, sn-trace-resorbed, opaques
DS89004	Tf	pl, bt, hb, qtz-resorbed, sn, opaques
DS89006	Tfm	pl, hb, bt, opaques
DS89012	Tf	pl, hb-altered, bt-altered, sn-resorbed, opaques
DS89014	Tf	pl, hb-altered, bt, cpx, sn-resorbed-trace, opaques
DS89015	Tf	pl, hb-altered, opaques
DS89028	Tsd	pl, hb, opaques
DY89-7	Tsd	pl, hb, bt, cpx, opaques
DY89-8	Tsd	pl, hb-altered, cpx, bt-trace, opaques
DY89-9	Tsd	pl, hb, bt, opaques
DS89016	Tsd	pl, hb-altered, bt, opaques
DS89017	Tsa	pl, cpx & opx, hb, altered, opaques
DS89019	Tsh	pl, hb-altered, cpx & opx, opaques
DS89029	Tsh	pl, hb, bt, cpx, opaques
DS89030	Tsh	pl, hb, bt, cpx & opx, (groundmass calcite alteration
DS89034	Tsd	pl, hb, bt, opaques
DS89035	Tsd	pl, hb, bt, opaques
88L-32	Tsi	pl,hb,px?, opaques $CaCO_3$, alteration, mafics altered
88L-34	Tsi	pl, px, hb, opaques
88L-36	Tsi	pl, hb, px, opaques, qtz-trace
88L-61	Tsi	pl, hb, opx,cpx, opaques
89L-129	Tsi	pl, cpx & opx-trace, hb-trace, opaques (trapped melt?
88L-31A	Tsa	pl, opx, cpx, hb-trace, opaques
88L-31B	Tsa	pl, hb, px, opaques
88L-31C	Tsh	pl, hb, px, opaques
88L-58	Tsd	pl,hb,px?,opaques,some feldspars are altered
88L-62A	Tsh	pl, hb, bt, px?, opaques (no thin section)
88L-62B	Tsh	pl, hb, biotite-trace, opaques
88L-62C	Tsd	pl, hb, opaques (no thin section)
88L-62D	Tsd	pl,hb,secondary quartz and calcite alteration
88L-62E	Tsd	pl,hb?,rock is slightly propylitized(no thin sect.)
88L-65	Tsh	pl, hb, cpx, opx-trace, opaques
88L-66	Tsh	pl, hb, bt, opaques
88L-70	Tsh	pl, cpx & opx, hb, opaques
89L-115	Tsh	pl, hb, bt, px-trace?, opaques
89L-122	Tsh	pl, hb, bt-trace, cpx-trace, opaques
89L-123	Tsd	pl, hb, cpx & opx, bt, opaques
89L-128	Tsm	pl, hb, cpx & opx, opaques
89L-130	Tsm	pl, hb, (opx & cpx)-trace amounts, opaques
89L-135A	Tsi	pl, bt, px, opaques
89L-135B	Tsi	pl, hb, opaques (mafics are altered)
89L-143	Tsi	pl-altered, hb-altered, opaques
89L-144	Tsi	pl-altered, hb-altered, bt, opaques
DY89-16	Tsh	pl, hb, cpx & opx, opaques
DY89-17	Tsa	pl, cpx & opx, hb, opaques
DY89-18	Tsh	pl, hb, bt, cpx & opx, opaques
DS89007	Tsh	pl, hb-altered, bt?-altered, opaques
DS89008	Tsh	pl, hb, bt, opaques
DS89009	Tsh	pl, hb, cpx, opaques
DS89010	Tsa	pl, cpx & opx, opaques
89L-136	Ttm	pl, hb, opaques
89L-137	Ttm	pl, hb, opaques
89L-138	Tsi	pl,hb, bt-trace, opaques
89L-140	Ttm	pl, hb, bt, opaques
89L-141	Ttm	pl, hb, bt, qtz, opaques
89L-147B	Tsi	pl,hb,bt trace, chlorite alteration
DY89-20	Ttm	pl, cpx & opx, opaques
DY89-21	Ttm	pl, cpx & opx, opaques
DY89-22	Ttm	pl, opx & cpx, opaques
DY89-24	Ttm	pl, hb, cpx & opx, opaques
DY89-24B	Ttm	pl, hb, cpx & opx, opaques
DY89-25	Ttm	pl, cpx & opx, hb, opaques
DY89-26	Ttm	pl, hb, cpx & opx, opaques
DY89-27	Ttm	pl, hb, opaques